

## Synthesis and characterization of FeNi<sub>3</sub> nanoparticles and their application as catalysts for penicillin G degradation in a Fenton-like reaction

Ayat Hossein Panahi<sup>a</sup>, Mohammad Kamranifar<sup>b</sup>, Mohammad Hadi Moslehi<sup>c</sup>, Susana Rodriguez-Couto<sup>d</sup>, Negin Nasseh<sup>e,\*</sup>

<sup>a</sup>*Social Determinant of Health Research Center, Birjand University of Medical Sciences, Birjand, Iran, email: ayatpanahi@yahoo.com*

<sup>b</sup>*Medical Toxicology and Drug abuse Research Center (MTDRC), Birjand University of Medical Sciences (BUMS), Birjand, Iran, email: mo.kamrani@yahoo.com*

<sup>c</sup>*Department of Mathematics, Payame Noor University, Tehran, Iran, email: mh\_moslehi@pnu.ac.ir*

<sup>d</sup>*Ikerbasque, Basque Foundation for Science, Maria Diaz de Haro 3, 48013 Bilbao, Spain, email: susanarodriguezcouto@gmail.com*

<sup>e</sup>*Social Determinants of Health Research Center, Faculty of Health, Department of Environmental Health Engineering, Birjand University of Medical Sciences, Birjand, Iran, email: Negin\_Nasseh@yahoo.com*

Received 16 March 2019; Accepted 3 November 2019

### ABSTRACT

In the present study, FeNi<sub>3</sub> magnetic nanoparticles were synthesized using a co-precipitation method and characterized by X-ray diffraction (XRD), field emission scanning electron microscopy (FESEM) and vibrating sample magnetometry (VSM). Further, the synthesized nanoparticles were applied to penicillin G (PG) degradation in a Fenton-like reaction. The effect of different parameters such as pH (3–11), nanoparticle dose (0.1–1 g/L), PG concentration (10–100 mg/L), reaction time (5–180 min) and the concentration of peroxide hydrogen (50–200 mg/L) were investigated on PG degradation by the synthesized nanoparticles. According to the results obtained by the XRD spectra and the Scherrer equation the average size of the synthesized nanoparticles was 41 nm. The FESEM image revealed that the synthesized nanoparticles had a high density due to their magnetic nature and the VSM analysis showed that the nanoparticles had a magnetic saturation of about 68.52 emu/g, indicating they were a super-paramagnetic material. As for the PG degradation, the removal rate of PG in 180 min for initial PG concentrations of 10, 20, 30, 50, 70, and 100 mg/L were 100%, 93.3%, 86.9%, 74.34%, and 58.85%, respectively, operating under optimum conditions (i.e. pH = 5, nanoparticle dose 1 g/L and H<sub>2</sub>O<sub>2</sub> concentration 150 mg/L). Also, it was found that PG degradation fitted the pseudo-first-order kinetics equation ( $R^2 > 0.9$ ). In addition, re-usability tests showed that after 4 cycles, only 6% of the nanoparticles were lost during the Fenton-like process. Finally, according to the results, it can be concluded that FeNi<sub>3</sub> magnetic nanoparticles in the Fenton-like process have a good effect on the removal of penicillin G.

*Keywords:* Penicillin G; Degradation; Magnetic nanoparticles; Kinetics; Fenton-like reaction

### 1. Introduction

Currently, many kinds of pharmaceuticals such as antibiotics are utilized in human and veterinary medicine for disease control. Antibiotics can be from synthetic or

natural origin [1,2]. The presence of  $\beta$ -lactam rings in the chemical structure of antibiotics is one of the factors of their classification. Accordingly, antibiotics are divided into two groups:  $\beta$ -lactam and non- $\beta$ -lactam. The 65 percent of all

\* Corresponding author.

antibiotics used worldwide are  $\beta$ -lactam antibiotics [3–5]. Penicillin G (PG) (benzylpenicillin with a  $\beta$ -lactam ring) is a broad-spectrum  $\beta$ -lactam antibiotic produced by fungi belonging to the genus *Penicillium* and utilized as a medicine for the treatment of bacterial gastro-intestinal and systemic infections. PG has the highest antimicrobial activity against pathogenic bacteria among all natural antibiotics, it is very sensitive to heat and is considered as a weak acid ( $pK_a = 2.75$ ) [6,7].

According to different studies, antibiotics reach the aquatic environment from effluents of various sources such as those generated by the pharmaceutical industry, domestic, hospital and laboratory activities because conventional wastewater treatment plants are not able to remove them [7–11]. The presence of antibiotics in the water bodies has undesirable effects including toxicity for the living beings, expansion of resistance in pathogenic bacteria and the risk of mutagenesis and carcinogenesis in humans and other creatures. Hence, these compounds should be removed from the effluents before being discharged into the environment [12].

In the last decade, among the different available methods for pollutant removal the advanced oxidation processes (AOPs) have been used comprehensively in the removal of non-biodegradable compounds such as medicines and antibiotics [12–15]. AOPs are processes in which due to the production of highly reactive radicals, especially hydroxyl radicals that have an oxidation potential from 2 to 2.8 electron volts oxidize organic chemical compounds non-selectively in aqueous solution [12,14–18]. Among such processes, the Fenton process results from the combination of hydrogen peroxide ( $H_2O_2$ ) and the ferrous ion ( $Fe^{2+}$ ) in acidic media. This process does not require any special equipment, and the iron salts and hydrogen peroxide used are economical and environmentally friendly. The Fenton process has shown high efficiency in the degradation of organic pollutants [15,19–21]. However, it presents several drawbacks such as the production of considerable amounts of sludge, the use of costly oxidants, a limited pH range, and the need for a continuous supply of  $Fe(II)$  [20,21].

Hence, to overcome these limitations, Fenton-like processes which consist in replacing the  $Fe(II)$  by other catalysts a nano-catalyst has been suggested [22]. Fenton-like processes resolve the problems related to the product of ferric iron and sludge, as well as in contrast to the homogeneous Fenton process, Fenton-like process can be applied in a wide range of pH. Accordingly, several materials have been recently applied as catalysts such as  $FeNi_3$ ,  $Mn_3O_4$ , clay and zeolite coated with nanoparticles [22,23].  $FeNi_3$  nanoparticles have been considered by several researchers to remove organic matter due to their simplicity in synthesis and operation, effectiveness towards organic under a wide range of operational conditions, and easy recovery from aqueous solutions using a magnetic field [23–25]. In the several studies conducted by Nasseh et al. [23], Bokare et al. [26], Zelmanov et al. [27], Khodadadi et al. [25] and Yang et al. [28] were utilized Fenton-like process in the removal of organic compounds.

The aim of this study was the synthesis of  $FeNi_3$  nanoparticles to be applied in the degradation of the antibiotic penicillin G in a Fenton-like process.

## 2. Materials and methods

### 2.1. Chemicals

The penicillin G used in the present study was manufactured by Sigma-Aldrich (Germany) and its chemical characteristics are given in Table 1. Polyethylene glycol (PEG) (1.0 g MW 6000), iron chloride ( $FeCl_2 \cdot 4H_2O$ ), nickel chloride ( $NiCl_2 \cdot 6H_2O$ ), hydrazinium hydrate ( $N_2H_4 \cdot H_2O$  with a purity of 80%), hydrogen peroxide ( $H_2O_2$ ) and ethanol ( $C_2H_5OH$ ), were used to synthesize the  $FeNi_3$  nanoparticles and were purchased from Merck (Germany).

### 2.2. Synthesis of $FeNi_3$ nanoparticles

To synthesize  $FeNi_3$  nanoparticles, first, 1 g of PEG was dissolved in 180 mL of deionized water in a 500 mL volumetric flask. Then, 0.713 g of  $NiCl_2 \cdot 6H_2O$  and 0.1988 g of  $FeCl_2 \cdot 4H_2O$  were dissolved in 10 mL of distilled water separately and both solutions were added to the 500 mL volumetric flask containing the PEG solution. The solution pH was adjusted between  $12 \leq pH \leq 13$  using 1 M NaOH. Then, 9.1 mL of hydrazinium hydrate ( $N_2H_4 \cdot H_2O$ , 80% concentration) was added to the suspension. The reaction was subjected to intense mixing conditions for 24 h and during this time the pH was regularly controlled. After co-precipitation, the  $FeNi_3$  black nanoparticles were separated using a magnet N42 and washed several times by distilled water to reach a neutral pH. The separated nanoparticles were then vacuum dried at  $80^\circ C$  for 8 h [29].

### 2.3. Characterization of the synthesized nanoparticles

Field emission scanning electron microscopy (FESEM) and transmission electron microscopy (TEM) SIGMA VP-500 (ZEISS, Germany) was used to study the shape, diameter and surface detail of the synthesized nanoparticles. The magnetic properties of the synthesized nanoparticles were determined using a vibrating sample magnetometry (VSM) 7400 model. X-ray diffraction (XRD) spectrum (Pert Pro model X Panalytical, Netherland) was used to identify and characterize the crystalline size and structure of the synthesized nanoparticles.

### 2.4. Penicillin G (PG) degradation in a Fenton-like process

A stock solution of PG (1000 mg/L) in deionized water was prepared in a 1 L volumetric flask. All experiments were performed on 200 mL samples in a batch system at room temperature ( $24^\circ C \pm 2^\circ C$ ). To mix the samples, a magnetic stirrer was used at 350 rpm and the pH was adjusted with HCl and NaOH 1 N using a pH meter (Calimatic Co., Germany). Different variables affecting PG degradation were studied including pH (3, 5, 7, 9, and 11), nanoparticle dose (0.1, 0.2, 0.3, 0.5, 0.8, and 1 g/L), initial PG concentration (10, 20, 30, 50, 70, and 100 mg/L), reaction time (5, 10, 15, 30, 60, 90, and 180 min) and hydrogen peroxide concentration (50, 100, 150, and 200 mg/L).

The samples were collected at selected time intervals and the remaining PG concentrations were measured by a UV-vis spectrophotometer at a wavelength of 290 nm [30]. In samples containing hydrogen peroxide, 0.2 mL of  $Na_2S_2O_3$

solution 0.2 N was added immediately after sampling, to minimize the interference effect of H<sub>2</sub>O<sub>2</sub> on the results [23].

The following equation was used to calculate the efficiency of the adsorption process:

$$R(\%) = \left( \frac{PG_0 - PG_t}{PG_0} \right) \times 100 \quad (1)$$

where *R*, *PG*<sub>0</sub> and *PG*<sub>*t*</sub> are the PG removal in percentage, the initial PG concentration (mg/L) and the residual PG concentration (mg/L), respectively.

### 2.5. Kinetics study

Generally, the rate of heterogeneous catalytic reactions is described by the pseudo-first-order model using Langmuir–Hinshelwood (L–H) kinetic model.

$$\theta = -\frac{dc}{dt} = k_r \left( \frac{KC}{1+KC} \right) \quad (2)$$

In the above equation *θ*, *k<sub>r</sub>*, *C* and *K* are the reaction rate (mg/L min), the reaction rate constant, the pollutant concentration (mg/L), the uptake coefficient of pollutants, respectively.

For many diluted solutions with *K* << 1, the equation L–H (Eq. (2)) is simplified to a pseudo-first-order kinetic law.

$$-\frac{dc}{dt} = K_{obs} C \quad (3)$$

$$\ln \left( \frac{C}{C_0} \right) = -K_{obs} t \quad (4)$$

In this equation, *K*<sub>obs</sub> is the pseudo-first-order reaction constant (1/min), *t* is the reaction time (min), *C* is the residual concentration (mg/L), and *C*<sub>0</sub> is the initial concentration of the pollutant (mg/L) [31–33].

## 3. Results and discussion

### 3.1. Characterization of the synthesized nanoparticles

FESEM, TEM, XRD, and VSM morphological analyses were performed to study the FeNi<sub>3</sub> magnetic nanoparticles.

In Fig. 1a the FESEM image of a FeNi<sub>3</sub> nanoparticle is shown. Based on the obtained micrograph from synthesized nanoparticle, it could be inferred that the average size of the FeNi<sub>3</sub> nanoparticles was 43.02 nm. Also, it could be observed that tended to agglomerate due to their magnetic nature. Consequently, the synthesized nanoparticles are condensed.

In the TEM image (Fig. 1b) the irregular structure of the FeNi<sub>3</sub> nanoparticles can be seen. In addition, adhesion between the particles is due to the high magnetic properties of particles.

To gather the required information about the crystallographic structures and approximate crystalline size of nanoparticles, XRD patterns in the range of 5°–80° were obtained. Thus, the XRD pattern of a FeNi<sub>3</sub> nanoparticle is

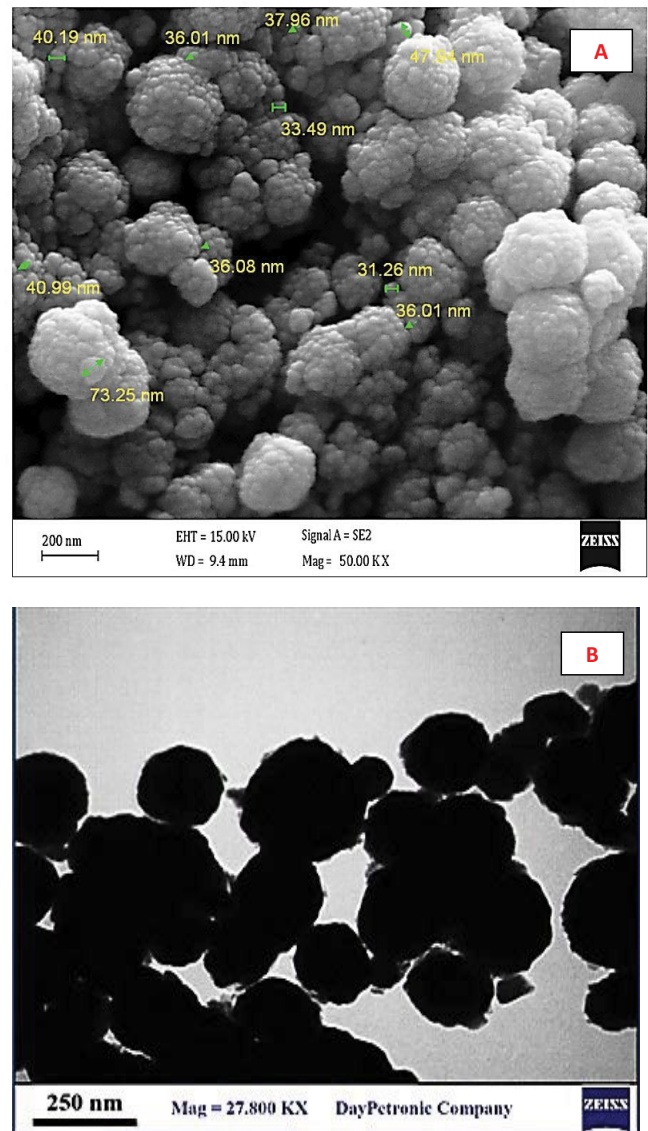


Fig. 1. FESEM (a) and TEM (b) image of FeNi<sub>3</sub> nanoparticle.

shown in Fig. 2a. The crystalline structure at 2θ = 75.81, 51.16, and 44.27 represents the structure of FeNi<sub>3</sub>. The crystalline size of the FeNi<sub>3</sub> nanoparticles were measured by applying the Scherrer equation:

$$D = \frac{0.98\lambda}{\beta \cos \theta} \quad (5)$$

where *D*, *β*, *θ* and *λ* are the particle diameter, the peak width at half-height, the diffraction angle at the peak and the wavelength of the X-ray device (λ = 0.1540) [21].

According to the Scherrer equation, the crystalline size of the synthesized nanoparticles were about 13 nm.

The magnetic properties of the FeNi<sub>3</sub> nanoparticles were studied by VSM at room temperature and the obtained results are presented in Fig. 2b.

In Fig. 2b one can observe that the nanoparticle has a magnetic saturation of 68.52 emu/g. Accordingly, it can be

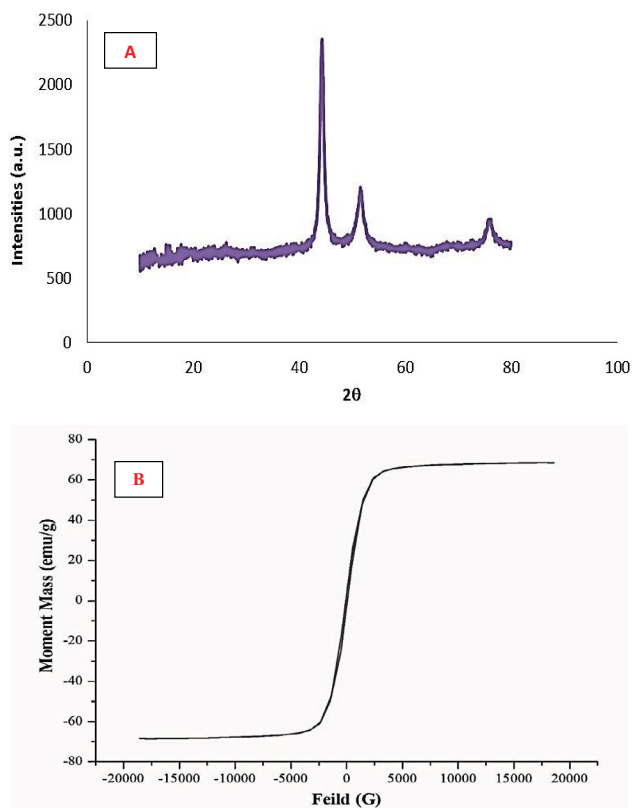


Fig. 2. XRD (a) and VSM (b) spectra of FeNi<sub>3</sub> nanoparticle.

concluded that the synthesized nanoparticles are super-paramagnetic and well dispersed in water. Therefore, these nanoparticles can be quickly and easily collected by the application of an external magnetic field and then with a slight shake can be dispersed again in water.

### 3.2. Adsorption of penicillin G (PG) by FeNi<sub>3</sub> nanoparticles

Before conducting the adsorption and Fenton-like experiments, the isoelectric point ( $pH_{ZPC}$ ) of the synthesized nanoparticles was determined to result to be 6.64 (Fig. 3a).

The adsorption experiments were conducted in batch at room temperature ( $24^{\circ}\text{C} \pm 2^{\circ}\text{C}$ ) for 60 min. Affecting variables including pH (3, 5, 7, 9, and 11), 0.20 g/L nanoparticle dose, and initial PG concentrations of 30 mg/L were investigated on PG adsorption. The results showed that the pH plays an important role in the adsorption process for a PG concentration of 30 mg/L and an adsorbent dose of 0.20 g/L. Thus, under the above-mentioned conditions at pH 3, 5, 7, 9, and 11, the removal percentage of PG was 22.86, 31.48, 18.96, 14.76, and 9.72 respectively. These results can be explained taking in to account the surface charge of FeNi<sub>3</sub> nanoparticles (6.64) and the  $pK_a$  of PG (Table 1). Thus, at a solution pH below the  $pH_{ZPC}$  the surface of the adsorbent is positively charged and attract anions from the solution. When the solution pH is higher than the  $pH_{ZPC}$  the surface of the adsorbent is negatively charged and attracts cations from the solution. In the present study, a lower pH is favorable for PG removal by FeNi<sub>3</sub> nanoparticles because at low pH the number of positively charged sites increases favoring

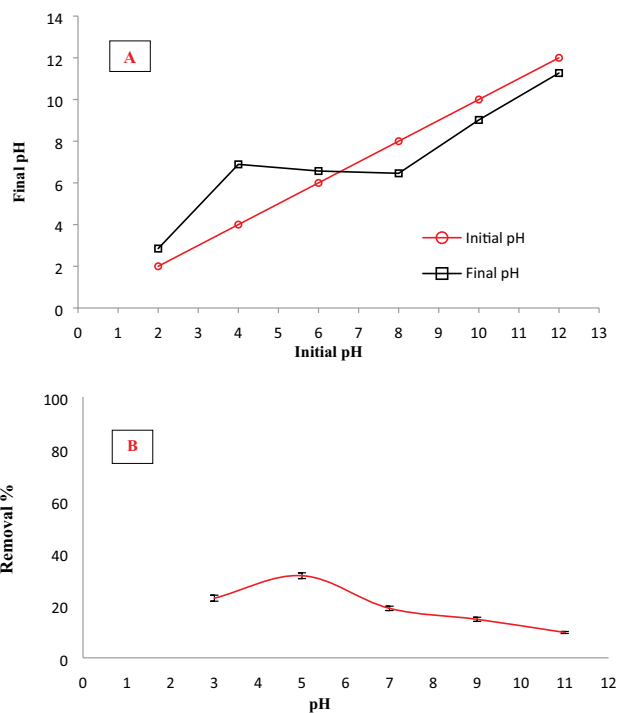


Fig. 3. Plot of  $pH_{ZPC}$  determination of FeNi<sub>3</sub> nanoparticle (a) and effect of pH on PG adsorption (b) (adsorbent dose = 0.2 g/L, PG concentration = 30 mg/L, and contact time of 60 min).

the adsorption of the negatively charged PG ions. PG has a negative charge at pH values higher than  $pH = 3$  due to its  $pK_a$ . Therefore, according to the results obtained (Fig. 3b), the highest percentage of PG adsorbed on FeNi<sub>3</sub> nanoparticles occurred at  $pH = 3-5$  due to the increase in electrostatic force between the adsorbent and adsorbate [20].

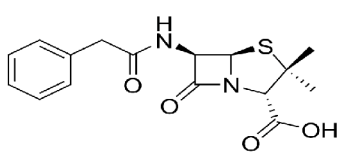
Increasing nanoparticle dose, the adsorption rate increased, because there are more adsorption sites available. Increasing the initial concentration of PG, the adsorption capacity was reduced due to the adsorption sites become occupied [23,25]. Another reason for this phenomenon is the saturation of the adsorbent surface at high concentrations of PG [23].

### 3.3. Penicillin G degradation in a Fenton-like process

#### 3.3.1. Effect of pH

For adsorption and degradation of organic pollutants in aqueous solutions, pH plays an important role in the solubility of PG antibiotics as well as its superficial charge. Therefore, we studied the effect of pH on the degradation of PG using FeNi<sub>3</sub> nanoparticles as catalysts in a Fenton-like process. The obtained results are shown in Fig. 4. As shown, by increasing pH value the efficiency of PG degradation reduced, so that the removal percentage of PG at pH of 3, 5, 7, 9, and 11 was, 54.67%, 70.48%, 47.85%, 42.98%, and 36.5% respectively operating at 20 mg/L initial PG concentration, 150 mg/L of hydrogen peroxide, 0.2 g/L nanoparticle dose and a reaction time of 60 min. The obtained results suggest that in a Fenton-like process, the degradation effectiveness

Table 1  
Structure and physical and chemical properties penicillin G

Structure	
	
Formula	$C_{16}H_{18}N_2O_4S$
Molecular weight	356.37 g/mol
Another name	Benzylpenicillin
Boiling point	209–212
pKa	2.74
Density	1.41 g/cm <sup>3</sup>
Solidity in water	100 mg/mL
Storage temperature	2°C–8°C
Elimination half-life	30 min
Protein binding	60%

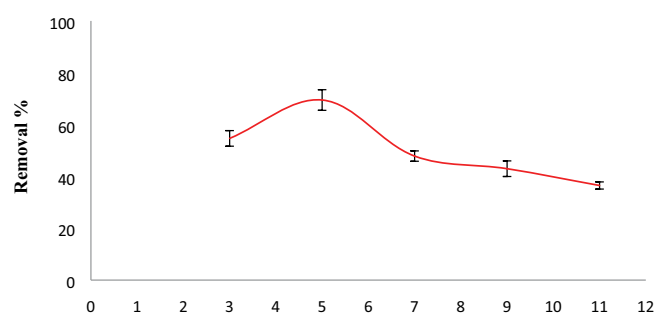


Fig. 4. Effect of pH on PG degradation of in Fenton-like process (catalyst dose = 0.2 g/L, PG concentration = 30 mg/L,  $H_2O_2$  concentration = 150 mg/L, and reaction time of 60 min).

by the synthesized nanoparticles was higher at acidic pH than at neutral and alkaline pH values [34]. The ionized iron in the samples may be combined with  $OH^-$  groups and precipitate as iron hydroxide [6]. Also, due to the reduction of hydroxyl radical activity in alkaline media,  $FeNi_3$  catalytic capacity reduces. Therefore, at alkaline pH, PG removal is mainly due to adsorption on the nanoparticles, and the proton deficiency causes the stopping of Fenton-like reaction. Moreover, at pH lower than the  $pH_{ZPC}$ , the  $FeNi_3$  surface charge is positive, under these conditions,  $H^+$  increases at the surface of the catalyst and thus the catalyst level becomes more hydrated [30]. The results of the studies performed by Norzaee et al. [35] and Wang et al. [36] are consistent with the results of the present study.

### 3.3.2. Effect of catalyst concentration

In Fig. 4 the rate of PG catalytic degradation in a heterogeneous  $FeNi_3/H_2O_2$  (Fenton-like) system at different concentrations of the nano-catalyst is shown. The experiments were performed at pH = 5, 150 mg/L  $H_2O_2$  concentration, 30 mg/L PG concentration and various doses of  $FeNi_3$  nanoparticles (0.1–1 g/L). As shown in Fig. 5, increasing the

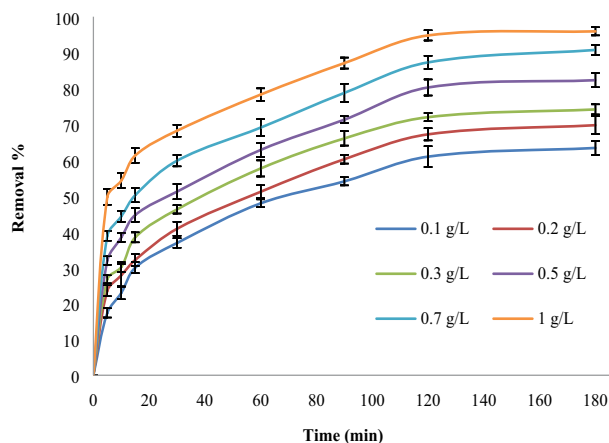


Fig. 5. Effect of catalyst dose on PG degradation in Fenton-like process (pH = 5, PG concentration = 30 mg/L and  $H_2O_2$  concentration = 150 mg/L).

dose of nanoparticles in the process led to an increase in the removal percentage of PG, so that the removal efficiency at 0.1 and 1 g/L of  $FeNi_3$  nanoparticles was 53.39% and 95.91% respectively. While in the presence of 150 mg/L  $H_2O_2$  alone the removal percentage of PG was much lower (i.e. 24.39% after 180 min). The reason for the significant increase in the removal percentage of PG using  $FeNi_3$  nanoparticles in the presence of  $H_2O_2$  can be explained by the fact that the active catalyst sites increase for the decomposition of hydrogen peroxide with increasing catalyst dose, which increases the hydroxyl free radical [28,37].

### 3.3.3. Effect of PG concentration

In this section, the effect of the initial concentration of PG in the range from 10 to 100 mg/L on PG removal was investigated keeping the other variables constant (pH = 5, catalyst dose 1 mg/L and hydrogen peroxide concentration 150 mg/L). As shown in Fig. 6, the removal percentage decreased by increasing PG concentration, so that the removal percentage at the initial concentration of 10 and 100 mg/L was 100% and 53.45% after 180 min, respectively. This reduction in PG removal could be because of the catalyst, contact time, the concentration of hydrogen peroxide and pH are the same, so at all concentrations, hydroxyl radical produced to remove penicillin G is the same. Therefore, it is logical that the removal of the antibiotics at lower concentrations is higher than the higher concentrations. On the other hand, on the surface of the synthesized nano-catalyst at higher concentrations, penicillin G molecules are more adsorbed and, consequently, in the reaction with hydroxyl radicals, the increase in penicillin G adsorption will have an inhibitory effect [38,39].

### 3.3.4. Effect of $H_2O_2$ concentration

We studied the effect of hydrogen peroxide concentration (in the range of 50–200 mg/L) as an oxidizing agent on the Fenton-like process ( $FeNi_3/H_2O_2$ ) on PG removal keeping the other variables constant (catalyst dose 1 g/L, pH = 5, PG



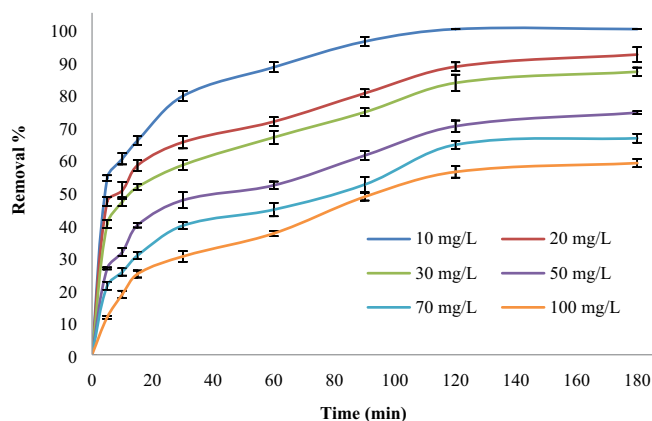
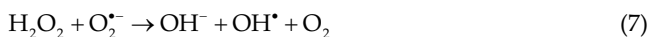


Fig. 6. Effect of initial concentration on PG degradation in Fenton-like process (pH = 5, catalyst dose = 0.1 g/L and  $H_2O_2$  concentration = 150 mg/L).

concentration 30 mg/L). The obtained results are shown in Fig. 7. It should be noted that the selection of hydrogen peroxide concentration should be proportional to the type and concentration of pollutants to maintain its efficiency because an excessive amount of it leads to loss of hydroxyl free radical [1]. Many studies have shown that the addition of hydrogen peroxide to the Fenton-like catalytic processes led in most cases to an increase in the oxidation rates (Eqs. (6) and (7)).



One of the main reasons for increasing the efficiency of PG oxidation by increasing the concentration of hydrogen peroxide is the production of more free radicals. The concentration of hydrogen peroxide is a key factor in the degradation of organic materials in AOPs, including Fenton, which, if determined optimally for the process, can save costs and prevent the phenomenon of scavenger [39].

### 3.3.5. Kinetics study

In order to investigate the kinetics of PG degradation in a Fenton-like process using  $FeNi_3$  synthesized nano-catalysts, the experiments were performed under optimum (catalyst dose 1 g/L, pH = 5 and hydrogen peroxide concentration of 200 mg/L at different reaction times). The obtained results are presented in Fig. 8 and Table 2 and showed that the pseudo-first-order model was suitable for describing the rate of this reaction. In addition, the results showed that by increasing the concentration of PG, the reaction rate reduces. This can be due to the increase in the concentration of intermediate products, active hydroxyl radicals in the reaction [23,25].

### 3.3.6. Study of stability and reusability of the catalyst

Measuring the activity, stability and reuse of solid catalysts are important parameters. For this reason, the reusability of the synthesized  $FeNi_3$  nanoparticles for PG

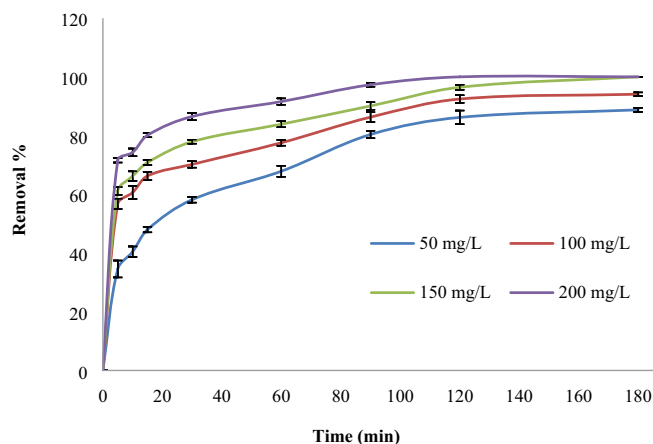


Fig. 7. Effect of  $H_2O_2$  concentration on PG degradation in Fenton-like process (pH = 5, catalyst dose = 0.1 g/L, and initial concentration = 30 mg/L).

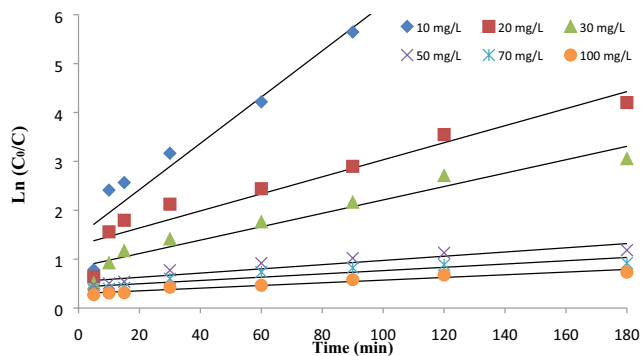


Fig. 8. Kinetic of PG degradation in Fenton-like process.

degradation in a Fenton-like process in 4 consecutive cycles was tested. The experimental conditions were as follows: PG concentration of 30 mg/L, catalyst dose of 1 g/L, contact time 180 min and pH = 5. At the end of each cycle, the catalysts were separated using an  $N_{42}$  magnet, and then they were washed several times with de-ionized water and vacuum dried at 80°C in an oven. The residual concentration of PG was measured at the end of each cycle, the results of which are shown in Fig. 9. According to the obtained results,  $FeNi_3$  nanoparticles are acceptable for reuse and recovery, so that after 4 cycles of PG degradation no significant reduction, and this reduction was only 6.14%, which could be due to reduced mass of nanoparticles during cycles. Regarding the results obtained,  $FeNi_3$  can be considered as a suitable catalyst in the developed Fenton-like process to decompose PG antibiotic.

## 4. Conclusion

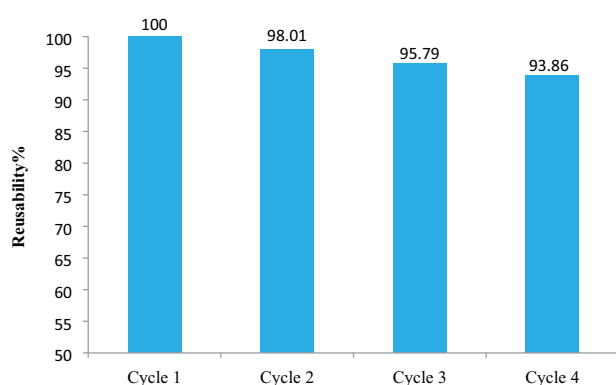
In this study, first,  $FeNi_3$  nanoparticles synthesized and their efficiency, alone and in combination with hydrogen peroxide (Fenton-like process), was investigated in the removal of penicillin G. According to morphological analysis and characterization of the synthesized nanoparticles, they were a super-paramagnetic nanoparticles. Also, this

Table 2

Pseudo-first-order kinetics parameters for degradation of penicillin G at various concentrations in FeNi<sub>3</sub>/H<sub>2</sub>O<sub>2</sub> Fenton process

Concentration (mg/L)	Equation	K <sub>0</sub> (min <sup>-1</sup> )	R <sup>2</sup>	t <sub>1/2</sub> (min)
10	Y = 0.0473x + 1.4756	47.3 × 10 <sup>-3</sup>	0.9416	14.65
20	Y = 0.0174x + 1.2898	17.4 × 10 <sup>-3</sup>	0.9684	39.82
30	Y = 0.0137x + 0.8416	13.7 × 10 <sup>-3</sup>	0.9818	50.58
50	Y = 0.0043x + 0.05432	4.3 × 10 <sup>-3</sup>	0.9489	161.162
70	Y = 0.0034x + 0.4296	3.4 × 10 <sup>-3</sup>	0.9648	203.82
100	Y = 0.0027x + 0.02977	2.7 × 10 <sup>-3</sup>	0.9285	256.67

$$t_{1/2} = 0.693/K_0$$

Fig. 9. Plot of stability and reusability of FeNi<sub>3</sub> catalyst in PG degradation using Fenton-like process.

synthesized material has a uniform distribution and a mean particle size of about 43 nm. The results of the adsorption process showed that the synthesized nanoparticles were not only suitable adsorbents for removing penicillin G from aqueous solution. According to the results of Fenton-like process, the highest rate of penicillin G degradation in the Fenton-like process was observed at pH = 5, nanoparticle dose of 1 g/L, PG concentration of 30 mg/L, H<sub>2</sub>O<sub>2</sub> concentration of 200 mg/L, and contact time 180 min. Operating under the above-mentioned conditions, the removal percentage of PG was 98.17%. The reaction kinetics in this study follows the pseudo-first-order equation ( $R^2 > 0.9$ ).

In addition, the results of the catalyst reusability tests showed that the synthesized nanoparticles had a high potential for recovery and reuse, such that the catalyst reduction was about 6.14% after 4 consecutive cycles in removal of PG. Finally, according to the results, it can be concluded that FeNi<sub>3</sub> nanoparticles in the presence of hydrogen peroxide are an efficient method to remove penicillin G from aqueous solutions because they can be easily separated from the reaction medium due to their super magnetic nature as well as due to their good sustainability as economic feasibility.

#### Acknowledgment

Authors express their gratitude to the colleagues at the research laboratory/Faculty of Health/Birjand University of Medical Sciences (Iran) for their spiritual support at various stages of this study.

#### References

- [1] R. Hirsch, T. Ternes, K. Haberer, K.-L. Kratz, Occurrence of antibiotics in the aquatic environment, *Sci. Total Environ.*, 225 (1999) 109–118.
- [2] P.E. Stackelberg, E.T. Furlong, M.T. Meyer, S.D. Zaugg, A.K. Henderson, D.B. Reissman, Persistence of pharmaceutical compounds and other organic wastewater contaminants in a conventional drinking-water-treatment plant, *Sci. Total Environ.*, 329 (2004) 99–113.
- [3] B.J. Hartman, A. Tomasz, Low-affinity penicillin-binding protein associated with beta-lactam resistance in *Staphylococcus aureus*, *J. Bacteriol.*, 158 (1984) 513–516.
- [4] K.-F. Kong, L. Schnepfer, K. Mathee, Beta-lactam antibiotics: from antibiosis to resistance and bacteriology, *APMIS*, 118 (2010) 1–36.
- [5] M.J. Torres, M. Blanca, J. Fernandez, A. Romano, A. de Weck, W. Aberer, K. Brockow, W.J. Pichler, P. Demoly, ENDA, EAACI Interest Group on Drug Hypersensitivity, Diagnosis of immediate allergic reactions to beta-lactam antibiotics, *Allergy*, 58 (2003) 961–972.
- [6] M. Dehghani, S. Nasser, M. Ahmadi, M.R. Samaei, A. Anushiravani, Removal of penicillin G from aqueous phase by Fe<sup>3+</sup>-TiO<sub>2</sub>/UV-A process, *J. Environ. Health Sci. Eng.*, 12 (2014) 56.
- [7] M.M. Hossain, J. Dean, Extraction of penicillin G from aqueous solutions: analysis of reaction equilibrium and mass transfer, *Sep. Purif. Technol.*, 62 (2008) 437–443.
- [8] R. Baccar, M. Sarrà, J. Bouzid, M. Feki, P. Blázquez, Removal of pharmaceutical compounds by activated carbon prepared from agricultural by-product, *Chem. Eng. J.*, 211–212 (2012) 310–317.
- [9] K. Kimura, H. Hara, Y. Watanabe, Removal of pharmaceutical compounds by submerged membrane bioreactors (MBRs), *Desalination*, 178 (2005) 135–140.
- [10] M. Sánchez-Polo, J. Rivera-Utrilla, G. Prados-Joya, M.A. Ferro-García, I. Bautista-Toledo, Removal of pharmaceutical compounds, nitroimidazoles, from waters by using the ozone/carbon system, *Water Res.*, 42 (2008) 4163–4171.
- [11] J.W. Peterson, L.J. Petrasky, M.D. Seymour, R.S. Burkhart, A.B. Schuiling, Adsorption and breakdown of penicillin antibiotic in the presence of titanium oxide nanoparticles in water, *Chemosphere*, 87 (2012) 911–917.
- [12] T.J. Al-Musawi, H. Kamani, E. Bazrafshan, A.H. Panahi, M.F. Silva, G. Abi, Optimization of the effects of physicochemical parameters on the degradation of cephalexin in sono-Fenton reactor by using Box-Behnken response surface methodology, *Catal. Lett.*, 149 (2019) 1186–1196.
- [13] E. Bazrafshan, T.J. Al-Musawi, M.F. Silva, A.H. Panahi, M. Havangi, F.K. Mostafapur, Photocatalytic degradation of catechol using ZnO nanoparticles as catalyst: optimizing the experimental parameters using the Box-Behnken statistical methodology and kinetic studies, *Microchem. J.*, 147 (2019) 643–653.
- [14] J. Jeong, W. Song, W.J. Cooper, J. Jung, J. Greaves, Degradation of tetracycline antibiotics: mechanisms and kinetic studies for

- advanced oxidation/reduction processes, *Chemosphere*, 78 (2010) 533–540.
- [15] M. Klavarioti, D. Mantzavinos, D. Kassinos, Removal of residual pharmaceuticals from aqueous systems by advanced oxidation processes, *Environ. Int.*, 35 (2009) 402–417.
- [16] N. Farhadian, R. Akbarzadeh, M. Pirsahab, T.-C. Jen, Y. Fakhri, A. Asadi, Chitosan modified N, S-doped TiO<sub>2</sub> and N, S-doped ZnO for visible light photocatalytic degradation of tetracycline, *Int. J. Biol. Macromol.*, 132 (2019) 360–373.
- [17] N. Rastkari, A. Eslami, S. Nasser, E. Piroti, A. Asadi, Optimizing parameters on nanophotocatalytic degradation of ibuprofen using UVC/ZnO processes by response surface methodology, *Pol. J. Environ. Stud.*, 26 (2017) 785–794.
- [18] S. Nasser, M.O. Borna, A. Esrafil, R.R. Kalantary, B. Kakavandi, M. Sillanpää, A. Asadi, Photocatalytic degradation of malathion using Zn<sup>2+</sup>-doped TiO<sub>2</sub> nanoparticles: statistical analysis and optimization of operating parameters, *Appl. Phys. A*, 124 (2018) 175.
- [19] I. Arslan-Alaton, F. Gurses, Photo-Fenton-like and photo-fenton-like oxidation of Procaine Penicillin G formulation effluent, *J. Photochem. Photobiol., A*, 165 (2004) 165–175.
- [20] S. Karthikeyan, V. Gupta, R. Boopathy, A. Titus, G. Sekaran, A new approach for the degradation of high concentration of aromatic amine by heterocatalytic Fenton oxidation: kinetic and spectroscopic studies, *J. Mol. Liq.*, 173 (2012) 153–163.
- [21] Karami, K. Sharafi, A. Asadi, A. Bagheri, F. Yosefvand, S.S. Charganeh, N. Mirzaei, A. Velayati, Degradation of Reactive Red 198 (RR198) from aqueous solutions by advanced oxidation processes (AOP): O<sub>3</sub>, H<sub>2</sub>O<sub>2</sub>/O<sub>3</sub> and H<sub>2</sub>O<sub>2</sub>/ultrasonic, *Bulg. Chem. Commun.*, 48 (2016) 43–49.
- [22] Z. Wan, J. Wang, Degradation of sulfamethazine antibiotics using Fe<sub>3</sub>O<sub>4</sub>-Mn<sub>3</sub>O<sub>4</sub> nanocomposite as a Fenton-like catalyst, *J. Chem. Technol. Biotechnol.*, 92 (2017) 874–883.
- [23] N. Nasseh, L. Taghavi, B. Barikbin, M.A. Nasser, A. Allahresani, FeNi<sub>3</sub>/SiO<sub>2</sub> magnetic nanocomposite as an efficient and recyclable heterogeneous fenton-like catalyst for the oxidation of metronidazole in neutral environments: adsorption and degradation studies, *Composites, Part B*, 166 (2019) 328–340.
- [24] S.-H. Hsieh, J.-J. Horng, Deposition of Fe-Ni nanoparticles on Al<sub>2</sub>O<sub>3</sub> for dechlorination of chloroform and trichloroethylene, *Appl. Surf. Sci.*, 253 (2006) 1660–1665.
- [25] M. Khodadadi, M. Ehrampoush, A. Allahresani, M. Ghanian, M. Lotfi, A. Mahvi, FeNi<sub>3</sub>@SiO<sub>2</sub> magnetic nanocomposite as a highly efficient Fenton-like catalyst for humic acid adsorption and degradation in neutral environments, *Desal. Wat. Treat.*, 118 (2018) 258–267.
- [26] A.D. Bokare, W. Choi, Review of iron-free Fenton-like systems for activating H<sub>2</sub>O<sub>2</sub> in advanced oxidation processes, *J. Hazard. Mater.*, 275 (2014) 121–135.
- [27] G. Zelmanov, R. Semiat, Iron (3) oxide-based nanoparticles as catalysts in advanced organic aqueous oxidation, *Water Res.*, 42 (2008) 492–498.
- [28] S.-T. Yang, W. Zhang, J. Xie, R. Liao, X. Zhang, B. Yu, R. Wu, X. Liu, H. Li, Z. Guo, Fe<sub>3</sub>O<sub>4</sub>@SiO<sub>2</sub> nanoparticles as a high-performance Fenton-like catalyst in a neutral environment, *RSC Adv.*, 5 (2015) 5458–5463.
- [29] M.A. Nasser, S.M. Sadeghzadeh, A highly active FeNi<sub>3</sub>-SiO<sub>2</sub> magnetic nanoparticles catalyst for the preparation of 4H-benzo[b]pyrans and Spirooxindoles under mild conditions, *J. Iran. Chem. Soc.*, 10 (2013) 1047–1056.
- [30] H. Pouretedal, N. Sadegh, Effective removal of amoxicillin, cephalixin, tetracycline and penicillin G from aqueous solutions using activated carbon nanoparticles prepared from vine wood, *J. Water Process. Eng.*, 1 (2014) 64–73.
- [31] A. Eslami, M.M. Amini, A.R. Yazdanbakhsh, A. Mohseni-Bandpei, A.A. Safari, A. Asadi, N, S co-doped TiO<sub>2</sub> nanoparticles and nanosheets in simulated solar light for photocatalytic degradation of non-steroidal anti-inflammatory drugs in water: a comparative study, *J. Chem. Technol. Biotechnol.*, 91 (2016) 2693–2704.
- [32] G. Safari, M. Hoseini, M. Seyedsalehi, H. Kamani, J. Jaafari, A. Mahvi, Photocatalytic degradation of tetracycline using nanosized titanium dioxide in aqueous solution, *Int. J. Environ. Sci. Technol.*, 12 (2015) 603–616.
- [33] A.-A. Salarian, Z. Hami, N. Mirzaei, S.M. Mohseni, A. Asadi, H. Bahrami, M. Vosoughi, A. Alinejad, M.-R. Zare, N-doped TiO<sub>2</sub> nanosheets for photocatalytic degradation and mineralization of diazinon under simulated solar irradiation: optimization and modeling using a response surface methodology, *J. Mol. Liq.*, 220 (2016) 183–191.
- [34] M. Tamimi, S. Qourzal, N. Barka, A. Assabbane, Y. Ait-Ichou, Methomyl degradation in aqueous solutions by Fenton's reagent and the photo-Fenton system, *Sep. Purif. Technol.*, 61 (2008) 103–108.
- [35] S. Norzaee, E. Bazrafshan, B. Djahed, F. Kord Mostafapour, R. Khaksefidi, UV activation of persulfate for removal of penicillin G antibiotics in aqueous solution, *Sci. World J.*, 2017 (2017) 6.
- [36] R. Wang, X. Liu, R. Wu, B. Yu, H. Li, X. Zhang, J. Xie, S.-T. Yang, Fe<sub>3</sub>O<sub>4</sub>/SiO<sub>2</sub>/C nanocomposite as a high-performance Fenton-like catalyst in a neutral environment, *RSC Adv.*, 6 (2016) 8594–8600.
- [37] S. Tian, Y. Tu, D. Chen, X. Chen, Y. Xiong, Degradation of Acid Orange II at neutral pH using Fe<sub>2</sub>(MoO<sub>4</sub>)<sub>3</sub> as a heterogeneous Fenton-like catalyst, *Chem. Eng. J.*, 169 (2011) 31–37.
- [38] B. Kakavandi, A. Takdastan, N. Jaafarzadeh, M. Azizi, A. Mirzaei, A. Azari, Application of Fe<sub>3</sub>O<sub>4</sub>@C catalyzing heterogeneous UV-Fenton system for tetracycline removal with a focus on optimization by a response surface method, *J. Photochem. Photobiol., A*, 314 (2016) 178–188.
- [39] R. Nosrati, A. Olad, R. Maramifar, Degradation of ampicillin antibiotic in aqueous solution by ZnO/polyaniline nanocomposite as photocatalyst under sunlight irradiation, *Environ. Sci. Pollut. Res.*, 19 (2012) 2291–2299.